ROYAL SOCIETY OF CHEMISTRY

## PAPER

Check for updates

# Cutting off the upstream and downstream costs for $CO_2$ electroreduction by upcycling fermentation emissions into ethanol†

Ruofan Sun,‡[ab] Jiwu Zhao‡[ab] and Xu Lu [ID] *[ab]

Electrochemical reduction of $CO_2$ ($CO_2$RR), when powered by renewables, opens up a new avenue to mitigate the greenhouse gas while producing value sustainably. Nevertheless, this technology has been largely limited by the high costs of the upstream $CO_2$ feed and downstream product separation. Here we report a hybrid bio-electrochemical system, integrating yeast fermentation with $CO_2$RR in one single cell, that upcycles the fermentation-emitted $CO_2$ into ethanol. We engineer a CuO−Ag tandem electrocatalyst with rationally designed CuO−Ag interfaces that pose minimal impact on the yeast, while efficiently converting $CO_2$ into ethanol against side reactions, such as hydrogen evolution and glucose reduction. We showcase the win−win model enabled by this hybrid system—the $CO_2$RR cost can be cut by 17.8% because the fermentation process provides a free, high-purity $CO_2$ source and free ethanol distillation and in return, the $CO_2$RR reduces the $CO_2$ emissions of fermentation and increases the final ethanol product concentration. This proof-of-concept procedure sheds light on a tempting possibility for a cost-effective $CO_2$ value chain.

*Dr Xu Lu obtained his BS and PhD degrees from the Department of Mechanical Engineering, University of Hong Kong in 2012 and 2017, respectively. He was then trained as a postdoctoral fellow in the Energy Sciences Institute, Yale University. Dr Lu joined King Abdullah University of Science and Technology (KAUST) as an Assistant Professor in Mechanical Engineering in March 2021. He established the Low-carbon*

**Xu Lu**

*Energy Conversion and Storage (LECS) Laboratory, which focuses on electrochemical upcycling of industrial high-pressure $CO_2$. So far, the LECS Laboratory has published original research articles in Nature Communications (3), Journal of the American Chemical Society, Angewandte Chemie, Chemical Engineering Journal, Journal of Energy Chemistry, etc., and generated two US provisional patents. The LECS Laboratory is also developing kilowatt-scale electrolyzers with industrial partners such as ACWA Power and Saudi Aramco.*

## Introduction

Renewable-driven production of value-added chemicals *via* electrochemical reduction of $CO_2$ ($CO_2$RR) holds promise to simultaneously benefit environmental sustainability and realize a low carbon footprint in manufacturing industry.[1–3] To date, the field has demonstrated high-yield and efficient production of multiple $CO_2$RR products, including carbon monoxide (CO), formic acid/formate (HCOOH or $HCOO^-$), methane ($CH_4$), methanol ($CH_3OH$), ethylene ($C_2H_4$), acetic acid/acetate ($CH_3$-COOH or $CH_3COO^-$), and ethanol ($CH_3CH_2OH$).[4–6] Converting $CO_2$ to ethanol is of particular importance because ethanol is a high-energy-density fuel additive that can facilitate cleaner combustion compared to conventional gasoline, such as the E85 ethanol fuel.[7–9] Ethanol also serves as the key chemical in pharmaceutical and cosmetic industries.[10,11] According to a report by GlobeNewswire, ethanol consumption in the European Union was estimated at approximately 4.8 million tons in 2021.[12]

Despite major advances, $CO_2$RR technology has been greatly challenged by its costly upstream and downstream processes.[13–15] On the one hand, the upstream feed of $CO_2$RR should be high-purity $CO_2$, due to the substantial energy and capital expenses required for direct electroreduction of impure

*[a] CCRC, Division of Physical Science and Engineering (PSE), King Abdullah University of Science and Technology (KAUST), Thuwal, 23955-6900, Kingdom of Saudi Arabia. E-mail: xu.lu@kaust.edu.sa*
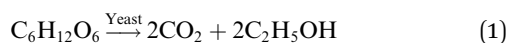
*[b] KAUST Solar Center (KSC), PSE, KAUST, Kingdom of Saudi Arabia*

† Electronic supplementary information (ESI) available. See DOI: https://doi.org/10.1039/d3ta07558c

‡ These authors contributed equally.

This journal is © The Royal Society of Chemistry 2024

*J. Mater. Chem. A*, 2024, **12**, 8429–8437 | 8429

$CO_2$.[16–18] The prevailing way to generate pure $CO_2$ gas is to capture $CO_2$ from point sources or air. Recent studies have described the possibility of integrating $CO_2$ capture with $CO_2RR$.[19–21] However, for now at least, $CO_2$ capture and recycling still incurs a high cost, which accounts to 9.3% of the capital expenditure (CapEx) and 8.3% of the operating expense (OpEx).[22–24] On the other hand, residue $CO_2$ and the electrolyte solution hold a large portion of the $CO_2RR$ effluent, and this necessitates downstream separation of products, which is another constraint of $CO_2RR$. Taking ethanol as an example again, the commonly used distillation apparatus not only leads to significant energy compensation, but also jeopardizes the cost effectiveness of the process—contributing approximately 3.9% CapEx and 2.3% OpEx of the overall $CO_2RR$ process.[13,24,25]

Bio-ethanol, produced from biomass through yeast fermentation, is the world's most popular ethanol supply, with a market size of $46.18 billion in 2022.[26,27] However, a typical bio-fermentation process produces bio-ethanol via reaction in an anaerobic environment:

$$C_6H_{12}O_6 \xrightarrow{\text{Yeast}} 2CO_2 + 2C_2H_5OH \qquad (1)$$

where significant amounts of $CO_2$ are emitted as a side product.[28] Different from fermentation in an aerobic reaction environment, where oxygen plays a part as a gas reactant, the emitted $CO_2$ in bio-ethanol fermentation has been proposed for use in food industry applications as a result of its high purity.[29] The global bio-ethanol yield in 2022 was 140 billion liters.[30] That means that approximately 106 million tons of $CO_2$ were emitted, leading to adverse environmental impacts and a heavy carbon penalty. It is estimated that the bio-ethanol manufacturing industry has been investing over $1.67–3.32 billion per year on the treatment of fermentation emissions.[31] However, fermentation $CO_2$ emission exhibits ultra-high purity (Fig. 1a),[32] and is thereby a perfect $CO_2RR$ input feed. Meanwhile, $CO_2$ from ambient air or other point sources, such as vehicle exhaust, oil refineries, steam reforming, ammonia production, iron and steel casting, and cement manufacture, usually come with significant amounts of impurities. In addition, the fermentation process consists of an ethanol distillation step, which could well serve the purpose of product separation for $CO_2RR$, if carefully designed.

Here we propose a fermentation–$CO_2RR$ hybrid that electrochemically converts high-purity fermentation-generated $CO_2$ into ethanol, which is then distilled together with the fermentation-produced bio-ethanol without extra cost. We tailor a CuO–Ag tandem catalyst with CuO–Ag interfaces that pose minimal influence on yeast activity while maintaining a reasonable faradaic efficiency (FE) for $CO_2$-to-ethanol conversion. In situ Raman studies show that the role of the CO intermediate on the CuO–Ag surface accelerates the C–C coupling process, reversibly suppressing side reactions such as hydrogen evolution and glucose reduction. Techno-economic analysis (TEA) indicates that our system not only cuts off the upstream and downstream expenses of $CO_2RR$ (that is, around 17.8% of the total $CO_2RR$ cost), but also benefits the fermentation by reducing $CO_2$ emissions. This proof-of-concept system

provides the possibility to address major bottlenecks for both $CO_2RR$ and fermentation.
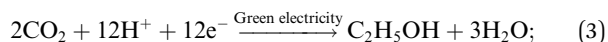
## Results

### Pathway design

$CO_2RR$ suffers from high costs of the (i) upstream $CO_2$ feed and (ii) downstream product separation, making it challenging for commercialization. We therefore propose a fermentation–$CO_2RR$ hybrid for $CO_2RR$ to take a free ride on the bio-fermentation process, which affords the possibility of cutting the two major costs of $CO_2RR$, by supplying high-purity $CO_2$ and providing free ethanol distillation. The proposed bio-electrochemical system (Fig. 1b) realizes a greener production of ethanol via a three-step pathway as below.

(i) Biomass fermentation as catalyzed by yeast, where ethanol is generated with high-purity $CO_2$ emission:

$$C_6H_{12}O_6 \xrightarrow{\text{Yeast}} 2CO_2 + 2C_2H_5OH; \qquad (2)$$

(ii) $CO_2RR$ powered by renewables, where the $CO_2$ emission is upcycled into ethanol:

$$2CO_2 + 12H^+ + 12e^- \xrightarrow{\text{Green electricity}} C_2H_5OH + 3H_2O; \qquad (3)$$

(iii) Ethanol distillation for the delivery of final product.

To confirm the cost effectiveness of the fermentation–$CO_2RR$ hybrid system, we performed TEA for $CO_2$ electroreduction to ethanol, assuming a base electricity cost of 0.02 $ per kW h, in line with the target set by US Department of Energy (DOE) for the year 2030.[33] TEA revealed that the $CO_2$ feed and the ethanol distillation accounted for 9.1% and 8.7% of the total $CO_2RR$ cost with an operating current density of 200 mA cm$^{-2}$ and ethanol FE of 50%—that is, 17.8% of the expense can be saved by our proposed system compared to a stand-alone $CO_2RR$ device (Fig. 1c).

To realize this proof-of-concept system, we first need to validate the $CO_2$ output from fermentation. We used 0.1 M glucose solution, as is commonly used in literature, as the fermentation feedstock for yeast to generate ethanol.[34,35] Despite the fact that liquids such as glycerol and organic acids may exist as side products, $CO_2$ was the only gas product from anaerobic bio-ethanol fermentation, as analyzed by gas chromatography (GC)—that is, almost 100% $CO_2$ purity (Fig. 2a).[36] After 25 h of fermentation, $CO_2$ became saturated, and the saturation state lasted for at least 500 h (Fig. 2b). This indicated the capability of the fermentation to supply sufficient $CO_2$ to $CO_2RR$ over a prolonged time. The pH value of the fermentation broth remained stable at 5.83 (Fig. 2c), which provides a weakly acidic environment that is beneficial to a high-carbon utilization efficiency during $CO_2RR$ because the otherwise neutral or alkaline environment at the cathode–electrolyte interface may lead to carbonate formation.[37–39] These observations authenticated the idea of feeding the fermentation $CO_2$ emissions to the $CO_2RR$, and motivated us to conduct the subsequent electrochemical experiments.

8430 | J. Mater. Chem. A, 2024, 12, 8429–8437

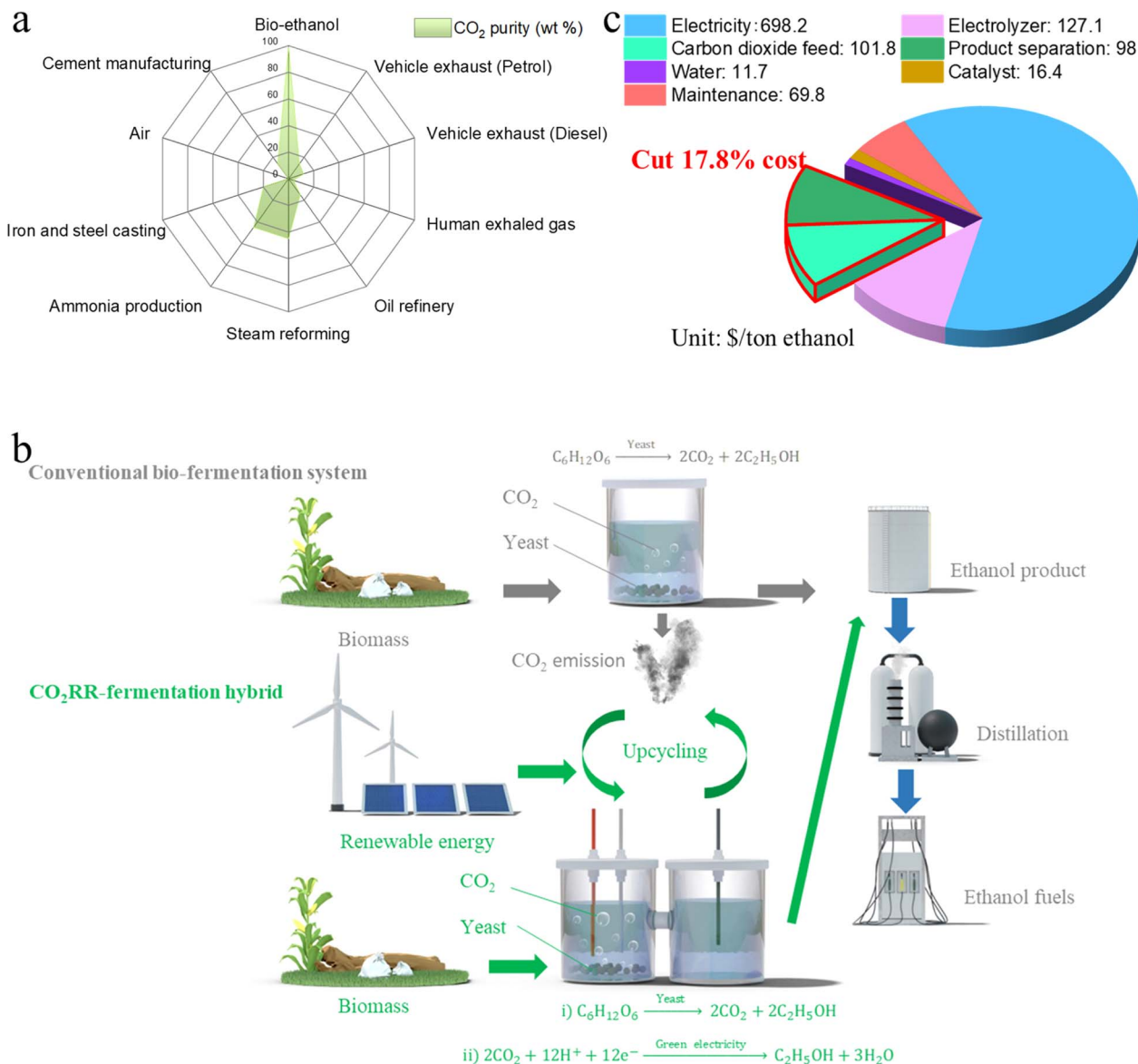This journal is © The Royal Society of Chemistry 2024

**Fig. 1** Schematics of TEA and the proposed hybrid system. (a) $CO_2$ purity (wt%) of various point sources and ambient air. (b) Schematic illustration of the fermentation–$CO_2$RR hybrid system. Bio-fermentation emits $CO_2$, which is upcycled into ethanol *via in situ* electrochemical conversion. This ethanol produced by the $CO_2$RR is then distilled together with the fermentation-generated bio-ethanol without extra cost. (c) Techno-economic analysis (TEA) of the proposed bio-electrochemical system *vs.* the conventional $CO_2$RR process for the production of ethanol. Our system saves on the costs of (i) acquiring high-purity $CO_2$ feed and (ii) separating the final product, thereby cutting the $CO_2$RR cost by at least 17.8%.

### CuO–Ag tandem catalyst for the fermentation–$CO_2$RR hybrid

Catalyst design strategies for $CO_2$RR to ethanol have been extensively studied, such as surface control, oxide modulation, oxophilicity engineering, *etc.*[40–42] Recently, tandem catalysts, especially Cu–Ag tandems, have demonstrated the capability of sequentially catalyzing $CO_2$-to-CO and CO-to-$C_2$ at reaction rates approaching industrial relevance.[43,44] Other homogeneously alloyed Cu-based bimetallic nanoparticles, as well as segmented tandem electrodes for increased CO coverage, can also enhance the $CO_2$-to-ethanol conversion.[45,46] For instance, CoPc@HC/Cu tandem electrode in acid $CO_2$RR exhibited a $C_{2+}$ FE of 90% and single-pass $CO_2$ conversion efficiency of 76%.[47] We

therefore sought to explore the possibility of designing a CuO–Ag tandem catalyst for our system (Fig. 3a). In brief, an Ag layer was first deposited on a carbon paper, followed by shadow mask-based Cu deposition to create 40 CuO–Ag interfaces in a 0.5 cm × 2 cm area. Of note, interface numbers higher than 40 were not prepared due to instrumentation constraints. Then, the electrode underwent galvanostatic anodic oxidation to form the final CuO–Ag tandem (Fig. 3b and S1†). The CuO–Ag interfaces were confirmed by transmission electron microscopy (TEM), electron energy loss spectroscopy (EELS), and energy-dispersive spectroscopy (EDS). Cu(111) and Ag(111) facets were delineated (Fig. 3c). EELS revealed the interface structure
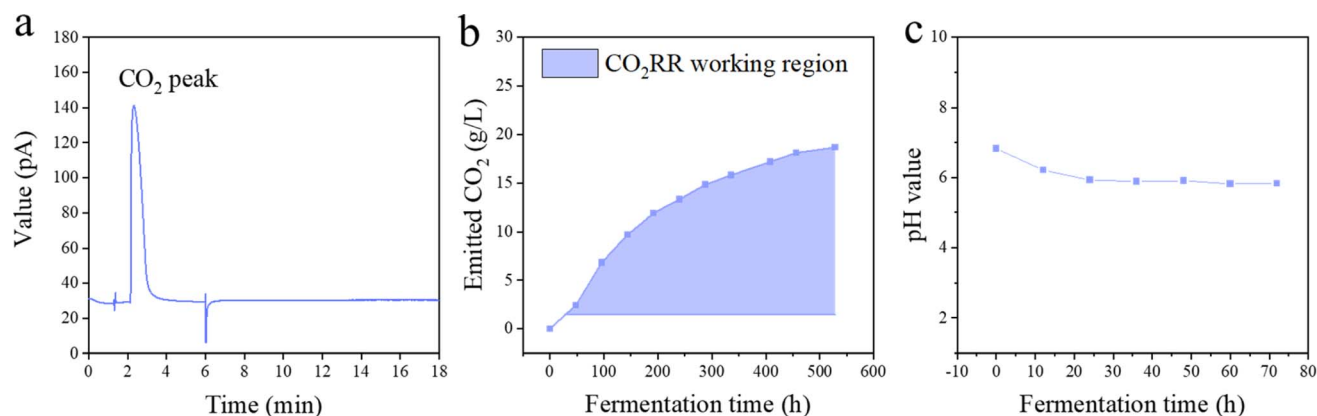
**Fig. 2** Fermentation emissions and broth condition. (a) Gas chromatography of fermentation-emitted $CO_2$. $CO_2$ is the only gas product. (b) Amount of fermentation-emitted $CO_2$ and (c) pH value of the fermentation broth over time.

at the nanoscale (Fig. 3d), while EDS uncovered the CuO–Ag at microscale (Fig. S2†). X-ray diffraction (XRD) patterns of the Cu segment of the as-prepared tandem electrode showed that CuO(110), CuO(111), and CuO (022) peaks increased during electrochemical oxidation, while those of Cu(111) and Cu(200) decreased over time (Fig. 3e), which implies the formation of CuO.[48] This was confirmed using Raman spectroscopy, which showed the characteristic peaks of CuO at 282, 330, and 616 $cm^{-1}$. Consistent with the literature, CuO exhibited a nanoplate morphology, while Ag appeared as nanoparticles (Fig. 3g and S3†).[49]
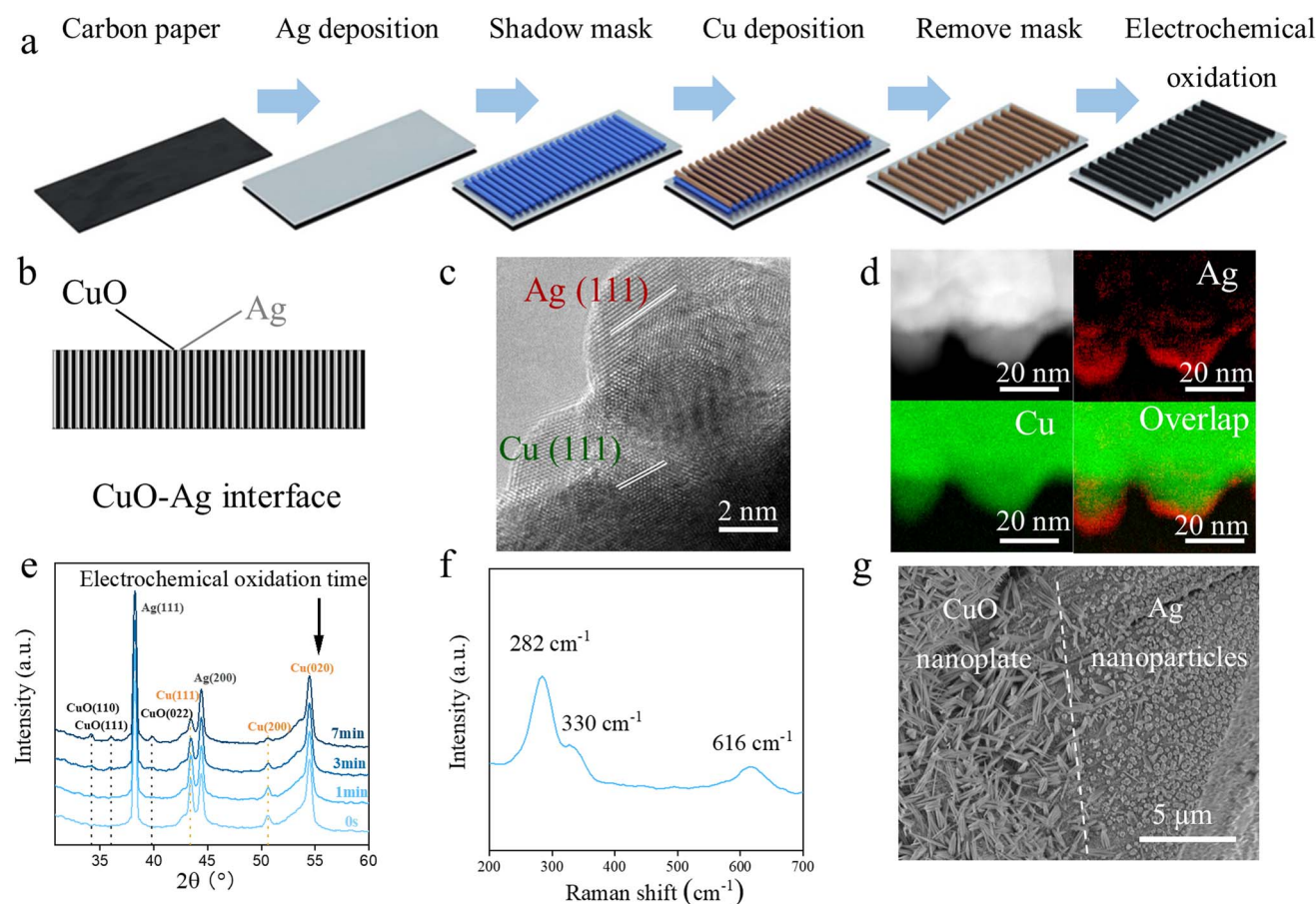


**Fig. 3** CuO–Ag tandem catalyst. Schematic of (a) the CuO–Ag tandem electrode synthesis and (b) the CuO–Ag interfaces. (c) HR-TEM and (d) EELS elemental mapping of the CuO–Ag interface. (e) XRD patterns of CuO–Ag over the electrochemical oxidation time. (f) Raman spectroscopy and (g) SEM of the CuO segment after oxidation.

**8432** | *J. Mater. Chem. A*, 2024, **12**, 8429–8437

This journal is © The Royal Society of Chemistry 2024

We then retrofitted a conventional fermentation system into an H-type hybrid cell that is compatible with $CO_2RR$—the cathode compartment contained 0.1 M glucose (a typical fermentation broth) and the anode compartment was filled with 0.5 M $KHCO_3$ aqueous solution (Fig. 4a). Nevertheless, the fermentation broth cannot provide the necessary electrochemical reaction conditions—the low electrolyte concentration resulted in sluggish adsorption of $OH^-$ on the catalyst surface, and increased both the charge transfer resistance ($R_{ct}$) and the electrical double layer (EDL) thickness.[50,51] Consequently, the $CO_2RR$ current density was limited below 8.85 mA $cm^{-2}$ at cathode potentials as negative as $-1.6$ V vs. the reversible hydrogen electrode (RHE) (Fig. 4b). To accommodate a reasonably high $CO_2RR$ reactivity, we attempted to add the most used cation, $K^+$, into the fermentation broth, such as $K_2CO_3$, KCl, and $KHCO_3$.[52–54] At a cathode potential of $-1.6$ V vs. RHE, the current density reached $-181$, $-152$, and $-161$ mA $cm^{-2}$ in 0.5 M $K_2CO_3$, 0.5 M KCl, and 0.5 M $KHCO_3$ glucose solutions, respectively, which is significantly higher than those in 0.1 M glucose, as suggested by linear sweep voltammetry

(LSV) curves (Fig. 4b). However, the addition of carbonate and bicarbonate anions resulted in an adverse impact on fermentation by tuning the pH towards alkaline, which was unfavorable for yeast activity,[55] whereas adding KCl maintained the fermentation broth as a weak acid to facilitate the fermentation process (Fig. S4†).[56] This was further confirmed by weighing the fermentation $CO_2$ emissions, where 0.5 M KCl merely changed the amount of yeast-generated $CO_2$, while in the case of $K_2CO_3$ and $KHCO_3$ obvious degradation of yeast activity was shown (Fig. 4c).[57] Therefore, we selected 0.1 M glucose aqueous solution (0.5 M KCl) as the catholyte for the fermentation–$CO_2RR$ hybrid cell.

Rationally, more CuO–Ag interfaces in a fixed area should benefit the $CO_2$-to-CO and CO-to-ethanol tandem reaction.[58,59] To confirm this, we compared CuO–Ag interface numbers of 0 (i.e. CuO), 10, 20, 30, and 40. It was observed that increasing the interface number resulted in higher ethanol selectivity; at $-0.87$ V vs. RHE, the ethanol FE was improved from 14.4% on CuO to 27.7% on CuO–Ag (20), and eventually reached 42.7% on CuO–Ag (40). Similar phenomena hold for the ethanol
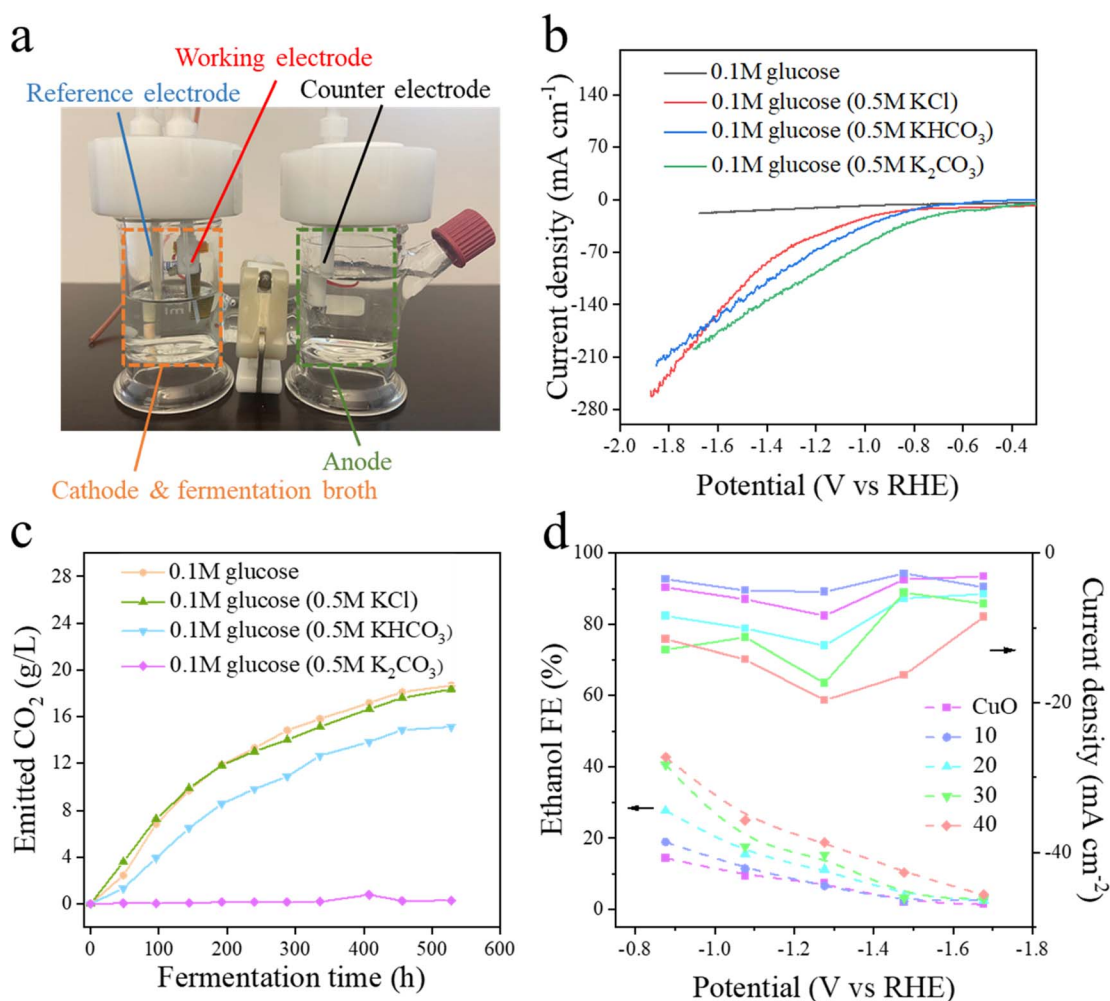


**Fig. 4** $CO_2RR$ performance in the fermentation–$CO_2RR$ hybrid cell. (a) Photo of the fermentation–$CO_2RR$ hybrid cell. (b) LSV curves of the CuO–Ag catalyst in different solutions. (c) Amount of fermentation $CO_2$ emissions in various glucose solutions. (d) Ethanol FEs and partial current densities with different CuO–Ag interface numbers (0, 10, 20, 30, and 40) in 0.1 M glucose (0.5 M KCl).
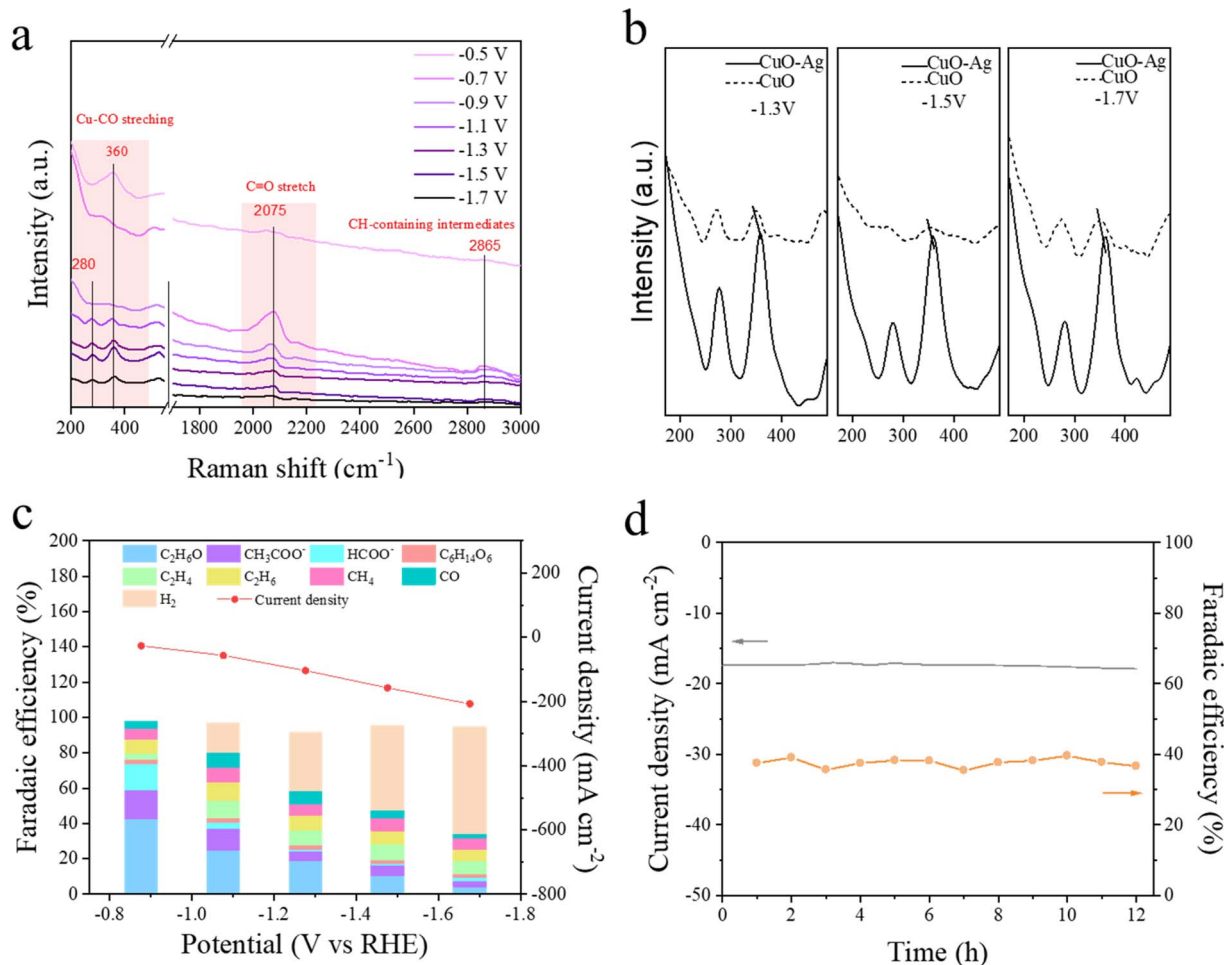
This journal is © The Royal Society of Chemistry 2024

J. Mater. Chem. A, 2024, 12, 8429–8437 | **8433**

Fig. 5 Enhanced ethanol production and proof-of-concept demonstration. (a) *In situ* Raman spectra acquired on CuO–Ag (40) under different potentials. (b) Comparison of *in situ* Raman spectra on CuO–Ag (40) and CuO catalysts at −1.3, −1.5, and −1.7 V *vs.* RHE. (c) FEs and current densities toward CO$_2$RR products, H$_2$, and sorbitol. (d) Prolonged operation of the CO$_2$RR–fermentation hybrid at −0.87 V *vs.* RHE. Pt foil was used as the anode. 0.1 M glucose (0.5 M KCl) solution was the electrolyte, and the CuO–Ag interface number was 40 unless otherwise stated.

productivity; at −1.27 V *vs.* RHE, the partial current density of ethanol was −8.4 mA cm$^{-2}$ on CuO, whereas it gradually increased to −19.6 mA cm$^{-2}$ on CuO–Ag (40) under the same conditions (Fig. 4d).

## Understanding the enhanced ethanol production for proof-of-concept

To gain insights into the improved ethanol yield at higher CuO–Ag interface numbers, *in situ* studies and density functional theory (DFT) calculations were conducted. Time-resolved X-ray diffractograms (Fig. S5†) revealed that CuO was reduced to Cu(111) and Cu(200) under CO$_2$RR condition, whereas the diffraction peaks of Ag barely changed, which is consistent with the X-ray photoelectron spectroscopy (XPS) results (Fig. S6†). This indicated that metallic Cu and Ag served as the dominant active sites during electrolysis, and prepared us to probe the key species distributions on the catalyst surface using *in situ* Raman spectroscopy. As mentioned above, the conversion of CO$_2$ to ethanol on a tandem catalyst proceeded *via* two steps: (i) CO formation, as catalyzed by Ag (Fig. S7 and S8†) and (ii) C–C

coupling, as catalyzed by Cu. Three regions in the Raman spectra were associated with the CO intermediates on the surface at negative potentials—the band at around 280 cm$^{-1}$ referred to the Cu–CO frustrated rotation mode,[58,60,61] the band at 360 cm$^{-1}$ was related to the Cu–CO stretch mode,[60,62] and the band at approximately 2075 cm$^{-1}$ can be ascribed to the C≡O stretch of the top-bound CO (Fig. 5a).[63,64] Compared to CuO, the band of the Cu–CO stretch was blue-shifted on the CuO–Ag interface at −1.3, −1.5, and −1.7 V *vs.* RHE (Fig. 5b and S9†), indicating a stronger binding of CO to the CuO–Ag interface.[65–67] The enhanced CO binding implied an enriched CO environment, which would promote the subsequent C–C coupling step, thereby resulting in a higher ethanol productivity.[68] DFT calculations confirm that the interface of Cu–Ag is more effective in ethanol generation (Fig. S10†). Compared to bare Cu, the free energy difference on the Cu–Ag interface is more gradual. For instance, the energy difference for adsorption of the second CO$_2$ is lower on the Cu–Ag interface (0.27 eV *vs.* 0.79 eV). Additionally, for C–C coupling, the Cu–Ag interface exhibits lower energy (1.09 eV *vs.* 1.46 eV).

8434 | *J. Mater. Chem. A*, 2024, **12**, 8429–8437

This journal is © The Royal Society of Chemistry 2024

To further rationalize our choice of a high CuO–Ag interface number, we examined the side reactions that occurred simultaneously with $CO_2RR$. In a typical $CO_2RR$ cell, the hydrogen evolution reaction (HER) is known to be the major competing reaction,[69–73] and it was slightly impacted by the CuO–Ag interface number because the active sites for the HER were essentially unchanged. In our $CO_2RR$–fermentation hybrid system, however, another competing reaction existed, namely, the glucose reduction reaction (GRR), where glucose is electrochemically reduced to sorbitol.[74] Compared to the HER, the GRR may pose a greater threat to $CO_2RR$ because both Cu and Ag have been reported to be active GRR catalysts.[75] Strikingly, our CuO–Ag (40) catalyst can effectively suppress the GRR: the GRR FE was 2.68% at −1.27 V vs. RHE, and this number even lower at 2.37% at −0.87 V vs. RHE (Fig. 5c). By stark contrast, the GRR FE increased to 2.91%, 3.51%, 3.71%, and 4.86% when the CuO–Ag interface number was 30, 20, 10, and 0, respectively (Fig. S11†). These observations verified our tandem catalyst design strategy, and, to the best of our knowledge, developing a $CO_2RR$ catalyst that can simultaneously suppress the GRR has never been reported. Finally, we sought to stably operate the proof-of-concept system. Our $CO_2RR$–fermentation hybrid exhibited a maximal ethanol FE of 42.7% at −0.87 V vs. RHE, with an overall current density of 27 mA cm$^{-2}$ (Fig. 5c). The partial current density towards ethanol reached 20 mA cm$^{-2}$, with an FE of 18.9% at −1.27 V vs. RHE. The current density and ethanol FE were well retained over the course of 12 h of chronoamperometric operation at −0.87 V vs. RHE (Fig. 5d). Ethanol was detected as the predominant liquid product (Fig. S12†).

## Conclusions

In summary, we have demonstrated a compelling bio-electrochemical system, combining yeast fermentation and $CO_2RR$, to upcycle the fermentation-emitted $CO_2$ into ethanol. Taking a free ride from the high-purity $CO_2$ emissions and ethanol distillation during fermentation, the $CO_2RR$–fermentation hybrid cuts the total $CO_2RR$ cost by 17.8%. A CuO–Ag tandem electrocatalyst with minimal impact on yeast was rationally designed, efficiently converting $CO_2$ to ethanol while suppressing side reactions, such as hydrogen evolution and glucose reduction. These results illustrate the possibility of a cost-effective $CO_2$ value chain for ethanol production. Further improvements are expected by optimizing the ethanol efficiency and yield through rational tandem electrode design, yeast selection, and system integration.

## Author contributions

X. L. supervised the project. X. L. and R. S. conceived the idea. R. S. synthesized and characterized the catalysts, and conducted electrochemical measurements. J. Z. made the DFT calculations. R. S. performed the fermentation experiments. R. S. and J. Z. carried out in situ Raman spectroscopy. R. S. conducted the TEA calculation. R. S. and X. L. wrote the manuscript. All authors discussed the results and assisted with the manuscript preparation.

## Conflicts of interest

The authors declare no competing interests.

## Acknowledgements

## References

1 O. S. Bushuyev, P. De Luna, C. T. Dinh, L. Tao, G. Saur, J. van de Lagemaat, S. O. Kelley and E. H. Sargent, *Joule*, 2018, **2**, 825–832.

2 Y. Wu, Z. Jiang, X. Lu, Y. Liang and H. Wang, *Nature*, 2019, **575**, 639–642.

3 R. G. Grim, Z. Huang, M. T. Guarnieri, J. R. Ferrell, L. Tao and J. A. Schaidle, *Energy Environ. Sci.*, 2020, **13**, 472–494.

4 G. Wang, J. Chen, Y. Ding, P. Cai, L. Yi, Y. Li, C. Tu, Y. Hou, Z. Wen and L. Dai, *Chem. Soc. Rev.*, 2021, **50**, 4993–5061.

5 W. Ma, X. He, W. Wang, S. Xie, Q. Zhang and Y. Wang, *Chem. Soc. Rev.*, 2021, **50**, 12897–12914.

6 D. Gao, R. M. Arán-Ais, H. S. Jeon and B. Roldan Cuenya, *Nat. Catal.*, 2019, **2**, 198–210.

7 A. Salvo and F. M. Geiger, *Nat. Geosci.*, 2014, **7**, 450–458.

8 P. Zhu and H. Wang, *Nat. Catal.*, 2021, **4**, 943–951.

9 C. E. Wyman and N. D. Hinman, *Appl. Biochem. Biotechnol.*, 1990, **24**, 735–753.

10 A. Duereh, H. Guo, T. Honma, Y. Hiraga, Y. Sato, R. Lee Smith Jr and H. Inomata, *Ind. Eng. Chem. Res.*, 2018, **57**, 7331–7344.

11 D. W. Lachenmeier, *J. Occup. Med. Toxicol.*, 2008, **3**, 1–16.

12 *EU Ethanol Market Report: Suppliers, Prices, Trends and Forecast to 2030*, IndexBox, 2022.

13 M. Jouny, W. Luc and F. Jiao, *Ind. Eng. Chem. Res.*, 2018, **57**, 2165–2177.

14 M. G. Kibria, J. P. Edwards, C. M. Gabardo, C. T. Dinh, A. Seifitokaldani, D. Sinton and E. H. Sargent, *Adv. Mater.*, 2019, **31**, 1807166.

15 J. M. Spurgeon and B. Kumar, *Energy Environ. Sci.*, 2018, **11**, 1536–1551.

16 P. Li, X. Lu, Z. Wu, Y. Wu, R. Malpass-Evans, N. B. McKeown, X. Sun and H. Wang, *Angew. Chem., Int. Ed.*, 2020, **59**, 10918–10923.

17 X. Lu, Z. Jiang, X. Yuan, Y. Wu, R. Malpass-Evans, Y. Zhong, Y. Liang, N. B. McKeown and H. Wang, *Sci. Bull.*, 2019, **64**, 1890–1895.

18 Y. Xu, J. P. Edwards, J. Zhong, C. P. O'Brien, C. M. Gabardo, C. McCallum, J. Li, C.-T. Dinh, E. H. Sargent and D. Sinton, *Energy Environ. Sci.*, 2020, **13**, 554–561.

19 G. Lee, A. S. Rasouli, B.-H. Lee, J. Zhang, Y. C. Xiao, J. P. Edwards, M. G. Lee, E. D. Jung, F. Arabyarmohammadi, H. Liu and E. Sargent, *Joule*, 2023, **7**, 1277–1288.

20 Y. Cheng, J. Hou and P. Kang, *ACS Energy Lett.*, 2021, **6**, 3352–3358.

This journal is © The Royal Society of Chemistry 2024

J. Mater. Chem. A, 2024, **12**, 8429–8437 | **8435**

21 A. J. Welch, E. Dunn, J. S. DuChene and H. A. Atwater, *ACS Energy Lett.*, 2020, **5**, 940–945.

22 M. T. Ho, G. W. Allinson and D. E. Wiley, *Energy Procedia*, 2009, **1**, 763–770.

23 A. Raksajati, M. T. Ho and D. E. Wiley, *Ind. Eng. Chem. Res.*, 2013, **52**, 16887–16901.

24 M. Ramdin, B. De Mot, A. R. Morrison, T. Breugelmans, L. J. Van Den Broeke, J. M. Trusler, R. Kortlever, W. De Jong, O. A. Moultos and P. Xiao, *Ind. Eng. Chem. Res.*, 2021, **60**, 17862–17880.

25 D. R. Sánchez, K. Khalilpour and A. F. Hoadley, *Sustainable Energy Fuels*, 2021, **5**, 5866–5880.

26 *Bioethanol Market (By Application: Transportation, Alcoholic Beverages, Cosmetics, Pharmaceuticals, Others; By Feedstock: Starch Based, Sugar Based, Cellulose-Based; By Fuel Generation: First Generation, Second Generation, Third Generation; By Blend: E5, E10, E15 to E70, E75 & E85, Others (E85 to E100)) – Global Industry Analysis, Size, Share, Growth, Trends, Regional Outlook, and Forecast 2022–2030, Report 2210*, Precedence Research, 2022.

27 *Ethanol fuel*, can be found under **https://en.wikipedia.org/wiki/Ethanol_fuel**, accessed April 2023.

28 F. Rodrigues, P. Ludovico and C. Leão, *Biodiversity and Eecophysiology of Yeasts*, 2006, pp. 101–121.

29 Q. Zhang, C.-L. Cheng, D. Nagarajan, J.-S. Chang, J. Hu and D.-J. Lee, *Appl. Energy*, 2017, **206**, 364–371.

30 I. Edeh, *Bioethanol Technologies*, 2021, p. 1.

31 J. K. Stolaroff, S. H. Pang, W. Li, W. G. Kirkendall, H. M. Goldstein, R. D. Aines and S. E. Baker, *Front. Energy Res.*, 2021, **9**, 639943.

32 H. Pilorgé, N. McQueen, D. Maynard, P. Psarras, J. He, T. Rufael and J. Wilcox, *Environ. Sci. Technol.*, 2020, **54**, 7524–7532.

33 DOE, can be found under **https://www.energy.gov/eere/solar/sunshot-2030**, accessed: October 2018.

34 A. F. Duro and R. Serrano, *Curr. Microbiol.*, 1981, **6**, 111–113.

35 A. Aminian and E. Motamedian, *Sci. Rep.*, 2023, **13**, 1165.

36 B. Maiorella, H. W. Blanch and C. R. Wilke, *Biotechnol. Bioeng.*, 1983, **25**, 103–121.

37 A. S. Varela, *Curr. Opin. Green Sustainable Chem.*, 2020, **26**, 100371.

38 J. A. Rabinowitz and M. W. Kanan, *Nat. Commun.*, 2020, **11**, 5231.

39 Y. Wu, K. Kamiya, T. Hashimoto, R. Sugimoto, T. Harada, K. Fujii and S. Nakanishi, *Electrochemistry*, 2020, **88**, 359–364.

40 Y. Zhao, L. Hao, A. Ozden, S. Liu, R. K. Miao, P. Ou, T. Alkayyali, S. Zhang, J. Ning, Y. Liang, Y. Xu, M. Fan, Y. Chen, J. E. Huang, K. Xie, J. Zhang, C. P. O'Brien, F. Li, E. H. Sargent and D. Sinton, *Nat. Synth.*, 2023, **2**, 403–412.

41 J. Li, A. Ozden, M. Wan, Y. Hu, F. Li, Y. Wang, R. R. Zamani, D. Ren, Z. Wang, Y. Xu, D.-H. Nam, J. Wicks, B. Chen, X. Wang, M. Luo, M. Graetzel, F. Che, E. H. Sargent and D. Sinton, *Nat. Commun.*, 2021, **12**, 2808.

42 M. Li, N. Song, W. Luo, J. Chen, W. Jiang and J. Yang, *Adv. Sci.*, 2023, **10**, 2204579.

43 P.-C. Chen, C. Chen, Y. Yang, A. L. Maulana, J. Jin, J. Feijoo and P. Yang, *J. Am. Chem. Soc.*, 2023, **145**, 10116–10125.

44 D. Wei, Y. Wang, C. L. Dong, Z. Zhang, X. Wang, Y. C. Huang, Y. Shi, X. Zhao, J. Wang and R. Long, *Angew. Chem.*, 2023, **135**, e202217369.

45 T. Zhang, J. C. Bui, Z. Li, A. T. Bell, A. Z. Weber and J. Wu, *Nat. Catal.*, 2022, **5**, 202–211.

46 L. Fan, C. Xia, F. Yang, J. Wang, H. Wang and Y. Lu, *Sci. Adv.*, 2020, **6**, eaay3111.

47 Y. Chen, X.-Y. Li, Z. Chen, A. Ozden, J. E. Huang, P. Ou, J. Dong, J. Zhang, C. Tian, B.-H. Lee, X. Wang, S. Liu, Q. Qu, S. Wang, Y. Xu, R. K. Miao, Y. Zhao, Y. Liu, C. Qiu, J. Abed, H. Liu, H. Shin, D. Wang, Y. Li, D. Sinton and E. H. Sargent, *Nat. Nanotechnol.*, 2023, **1**, 8.

48 Q. Lei, L. Huang, J. Yin, B. Davaasuren, Y. Yuan, X. Dong, Z.-P. Wu, X. Wang, K. X. Yao, X. Lu and Y. Han, *Nat. Commun.*, 2022, **13**, 4857.

49 W. Liu, P. Zhai, A. Li, B. Wei, K. Si, Y. Wei, X. Wang, G. Zhu, Q. Chen and X. Gu, *Nat. Commun.*, 2022, **13**, 1877.

50 S. S. Bhargava, F. Proietto, D. Azmoodeh, E. R. Cofell, D. A. Henckel, S. Verma, C. J. Brooks, A. A. Gewirth and P. J. Kenis, *ChemElectroChem*, 2020, **7**, 2001–2011.

51 M. König, J. Vaes, E. Klemm and D. Pant, *iscience*, 2019, **19**, 135–160.

52 J.-J. Li and Z.-C. Zhang, *Rare Met.*, 2022, **41**, 723–725.

53 X. Zhang, J. Li, Y.-Y. Li, Y. Jung, Y. Kuang, G. Zhu, Y. Liang and H. Dai, *J. Am. Chem. Soc.*, 2021, **143**, 3245–3255.

54 A. B. Moss, S. Garg, M. Mirolo, C. A. G. Rodriguez, R. Ilvonen, I. Chorkendorff, J. Drnec and B. Seger, *Joule*, 2023, **7**, 350–365.

55 Y. Lin, W. Zhang, C. Li, K. Sakakibara, S. Tanaka and H. Kong, *Biomass Bioenergy*, 2012, **47**, 395–401.

56 H. Zentou, Z. Z. Abidin, M. Zouanti and D. Greetham, *Int. J. Appl. Eng. Res.*, 2017, **12**, 5202–5506.

57 I. Jood, J. W. Hoff and M. E. Setati, *World J. Microbiol. Biotechnol.*, 2017, **33**, 1–11.

58 J. Li, H. Xiong, X. Liu, D. Wu, D. Su, B. Xu and Q. Lu, *Nat. Commun.*, 2023, **14**, 698.

59 C. Chen, Y. Li, S. Yu, S. Louisia, J. Jin, M. Li, M. B. Ross and P. Yang, *Joule*, 2020, **4**, 1688–1699.

60 C. Chen, X. Yan, S. Liu, Y. Wu, Q. Wan, X. Sun, Q. Zhu, H. Liu, J. Ma and L. Zheng, *Angew. Chem.*, 2020, **132**, 16601–16606.

61 J. Gao, H. Zhang, X. Guo, J. Luo, S. M. Zakeeruddin, D. Ren and M. Grätzel, *J. Am. Chem. Soc.*, 2019, **141**, 18704–18714.

62 J. Li, A. Ozden, M. Wan, Y. Hu, F. Li, Y. Wang, R. R. Zamani, D. Ren, Z. Wang and Y. Xu, *Nat. Commun.*, 2021, **12**, 2808.

63 F. Li, A. Thevenon, A. Rosas-Hernández, Z. Wang, Y. Li, C. M. Gabardo, A. Ozden, C. T. Dinh, J. Li and Y. Wang, *Nature*, 2020, **577**, 509–513.

64 G. Zhang, Z.-J. Zhao, D. Cheng, H. Li, J. Yu, Q. Wang, H. Gao, J. Guo, H. Wang and G. A. Ozin, *Nat. Commun.*, 2021, **12**, 5745.

65 A. Fielicke, P. Gruene, G. Meijer and D. M. Rayner, *Surf. Sci.*, 2009, **603**, 1427–1433.

66 X. Wang, Z. Wang, F. P. García de Arquer, C.-T. Dinh, A. Ozden, Y. C. Li, D.-H. Nam, J. Li, Y.-S. Liu, J. Wicks,

**8436** | *J. Mater. Chem. A*, 2024, **12**, 8429–8437

This journal is © The Royal Society of Chemistry 2024

Z. Chen, M. Chi, B. Chen, Y. Wang, J. Tam, J. Y. Howe, A. Proppe, P. Todorović, F. Li, T.-T. Zhuang, C. M. Gabardo, A. R. Kirmani, C. McCallum, S.-F. Hung, Y. Lum, M. Luo, Y. Min, A. Xu, C. P. O'Brien, B. Stephen, B. Sun, A. H. Ip, L. J. Richter, S. O. Kelley, D. Sinton and E. H. Sargent, *Nat. Energy*, 2020, **5**, 478–486.

67 C. Zhan, F. Dattila, C. Rettenmaier, A. Bergmann, S. Kühl, R. García-Muelas, N. r. López and B. R. Cuenya, *ACS Catal.*, 2021, **11**, 7694–7701.

68 R. B. Sandberg, J. H. Montoya, K. Chan and J. K. Nørskov, *Surf. Sci.*, 2016, **654**, 56–62.

69 A. Goyal, G. Marcandalli, V. A. Mints and M. T. Koper, *J. Am. Chem. Soc.*, 2020, **142**, 4154–4161.

70 X. Li, H. Zhang, Q. Hu, W. Zhou, J. Shao, X. Jiang, C. Feng, H. Yang and C. He, *Angew. Chem., Int. Ed.*, 2023, **62**, e202300478.

71 X. Li, C. Deng, Y. Kong, Q. Huo, L. Mi, J. Sun, J. Cao, J. Shao, X. Chen and W. Zhou, *Angew. Chem., Int. Ed.*, 2023, **62**, e202309732.

72 Q. Hu, K. Gao, X. Wang, H. Zheng, J. Cao, L. Mi, Q. Huo, H. Yang, J. Liu and C. He, *Nat. Commun.*, 2022, **13**, 3958.

73 C. Feng, M. Lv, J. Shao, H. Wu, W. Zhou, S. Qi, C. Deng, X. Chai, H. Yang and Q. Hu, *Adv. Mater.*, 2023, **35**, 2305598.

74 A. Bin Kassim, C. Rice and A. Kuhn, *J. Appl. Electrochem.*, 1981, **11**, 261–267.

75 Y. Kwon and M. T. Koper, *ChemSusChem*, 2013, **6**, 455–462.

This journal is © The Royal Society of Chemistry 2024

*J. Mater. Chem. A*, 2024, **12**, 8429–8437 | **8437**